

## Supplementary Materials for

### Two-miRNA–based finger-stick assay for estimation of absorbed ionizing radiation dose

Marshleen Yadav, Sagar Bhayana, Joseph Liu, Lanchun Lu, Jason Huang, Ya Ma, Zahida Qamri, Xiaokui Mo, Diviya S. Jacob, Shashaank T. Parasa, Noureen Bhuiya, Paolo Fadda, Meng Xu-Welliver, Arnab Chakravarti, Naduparambil K. Jacob\*

\*Corresponding author. Email: naduparambil.jacob@osumc.edu

Published 15 July 2020, *Sci. Transl. Med.* **12**, eaaw5831 (2020)

DOI: 10.1126/scitranslmed.aaw5831

#### The PDF file includes:

##### Materials and Methods

Fig. S1. *miR-150-5p* and *miR-23a-3p* expression in human blood cell subsets, serum, and mouse tissues.

Fig. S2. Normalizer *miR-23a-3p* is unaltered after exposure to high doses of whole thorax irradiation in mice and is secreted in nonexosomal fashion.

Fig. S3. Finger-stick assay benchmarking according to gender and age at baseline in humans.

Fig. S4. Comparison of dose response and sensitivity in mouse blood versus serum.

Fig. S5. Longitudinal evaluation of dose response in pediatric, young-adult, middle-aged, and geriatric mice.

Fig. S6. CBC in mice of different ages after exposure to a broader dose range.

Fig. S7. Comparison of miR-RAD with lymphocyte depletion and NLR.

Fig. S8. Dose response in immunocompetent, immunocompromised, immune-challenged, partial body exposure, and DNA repair–deficient mice.

Fig. S9. miR-RAD with CBC analysis after neutron irradiation in mice.

Fig. S10. An overview of the accuracy of miR-RAD in a broad dose range.

Fig. S11. Relative biological effectiveness of neutron with miR-RAD endpoint.

Fig. S12. ROC curves for absorbed dose >2 or >6 Gy using miR-RAD.

Table S1. Baseline  $C_t$  values of *miR-150-5p* and *miR-23a-3p* in finger-stick blood from healthy volunteers and venous blood from patients with leukemia.

Table S2. Overview of mouse samples including number of animals and sampling time points.

Table S3. Overview of human samples used for dose-response evaluation and controls.

Table S4. Comparison of uncertainty error with  $\Delta\Delta C_t$  versus normalized  $\Delta\Delta C_t$  in mice.

Table S5. Tabulation of actual dose versus estimated dose in mice.

Table S6. Tabulation of assay sensitivity and specificity at 0.5, 2, and 6 Gy cutoff.

**Other Supplementary Material for this manuscript includes the following:**

(available at [stm.sciencemag.org/cgi/content/full/12/552/eaaw5831/DC1](http://stm.sciencemag.org/cgi/content/full/12/552/eaaw5831/DC1))

Data file S1 (Microsoft Excel format). Primary data.

## Materials and Methods:

### Exosome isolation

Six hundred  $\mu\text{l}$  of serum separated from healthy volunteers was used for exosome isolation while 400  $\mu\text{l}$  of serum was kept for direct comparisons. PBS was added to 600  $\mu\text{l}$  of serum to make up to 10 ml for passing through 0.22 micron filter columns. The filtered serum was then subjected to ultracentrifugation (Optima L-90K, Beckman Coulter) at 100,000 x g for 1 hour at 4°C. The pellet was resuspended in 220  $\mu\text{l}$  of PBS, with 20  $\mu\text{l}$  used for NanoSight analysis. The remaining 200  $\mu\text{l}$  was used for miRNA isolation by Qiagen miRNeasy Kit.

### Complete Blood Count (CBC)

Blood samples were collected, without sedation, by submandibular bleed of approximately 50  $\mu\text{l}$  into a vacutainer (Microvette 100K3E) containing EDTA as an anti-coagulant for hematology. Samples were immediately processed on an automated CBC analyzer (HemaVet Analyzer, Drew Scientific Inc.) at Comparative Pathology and Mouse Phenotyping Shared Resources (CPMPSR) at OSU.

### Dose reconstruction

Prediction algorithms were derived based on experimental mouse data points from the training set with the help of SigmaPlot software. These algorithms were then used to integrate the data points (normalized  $\Delta\Delta\text{Ct}$ ) collected from mice exposed to various doses in a blinded fashion. The normalized  $\Delta\Delta\text{Ct} = 2^{-[(\text{Ct}_{miR-150-5p} - \text{Ct}_{miR-23a-3p})/\text{Ct}_{miR-23a-3p}]}$ . The information on reduction in uncertainty in dose prediction at different time points is shown in table S4 and detailed calculation in datafile S1.

### Calculation of Relative Biological Effectiveness (RBE)

Relative biological effectiveness for IND-spectrum neutron was calculated by plotting  $\text{Ln}\{\text{Fold Change } (miR-150-5p/miR-23a-3p)\}$  against gamma radiation doses and measuring the overlapping dose response of neutron at 1, 2, and 3 Gy gamma radiation, applying formula  $\text{RBE} = \text{Dose}_{\text{low-LET}}/\text{Dose}_{\text{high-LET}}$ . The RBE values generated further by another approach where *miR-150-5p* dose responses obtained from neutron-exposed animals were translated into dose calculation by applying prediction algorithms derived from gamma irradiation studies.

### miRNA Profiling

One hundred ng of total RNA extracted from whole PBMCs and purified cell subsets, and five ng of total RNA extracted from whole blood (WB) and RBC were used for human miRNA profiling using nCounter platform (NanoString Technologies, Inc.) following manufacturer's protocol. Amount of RNA used for nanoString profiling from WB and RBC preparations were reduced to minimize confounding issues such as signal saturation. Total RNA was isolated from blood cells purified from three different leukopaks and serum from three healthy volunteers. Raw counts from the nanoString assay were subjected to technical normalization using positive controls (spiked in the code-set to normalize the lane by lane variations), background corrections (measured with a set of probes designed for target transcripts that are absent), and ligation efficiency (with positives to measure ligase enzyme activity). Then the biological normalization of miRNAs was performed using geometric means of top 100 miRNAs on nSolver software (NanoString Technologies). Normalized counts were used to derive top 65 miRNAs, represented as heat- map, and box plots comparing *miR-150-5p* and *miR-23a-3p* in WB and PBMC cell subsets. Global mean normalization was applied to calculate the percentage abundance of different miRNAs in each sample.

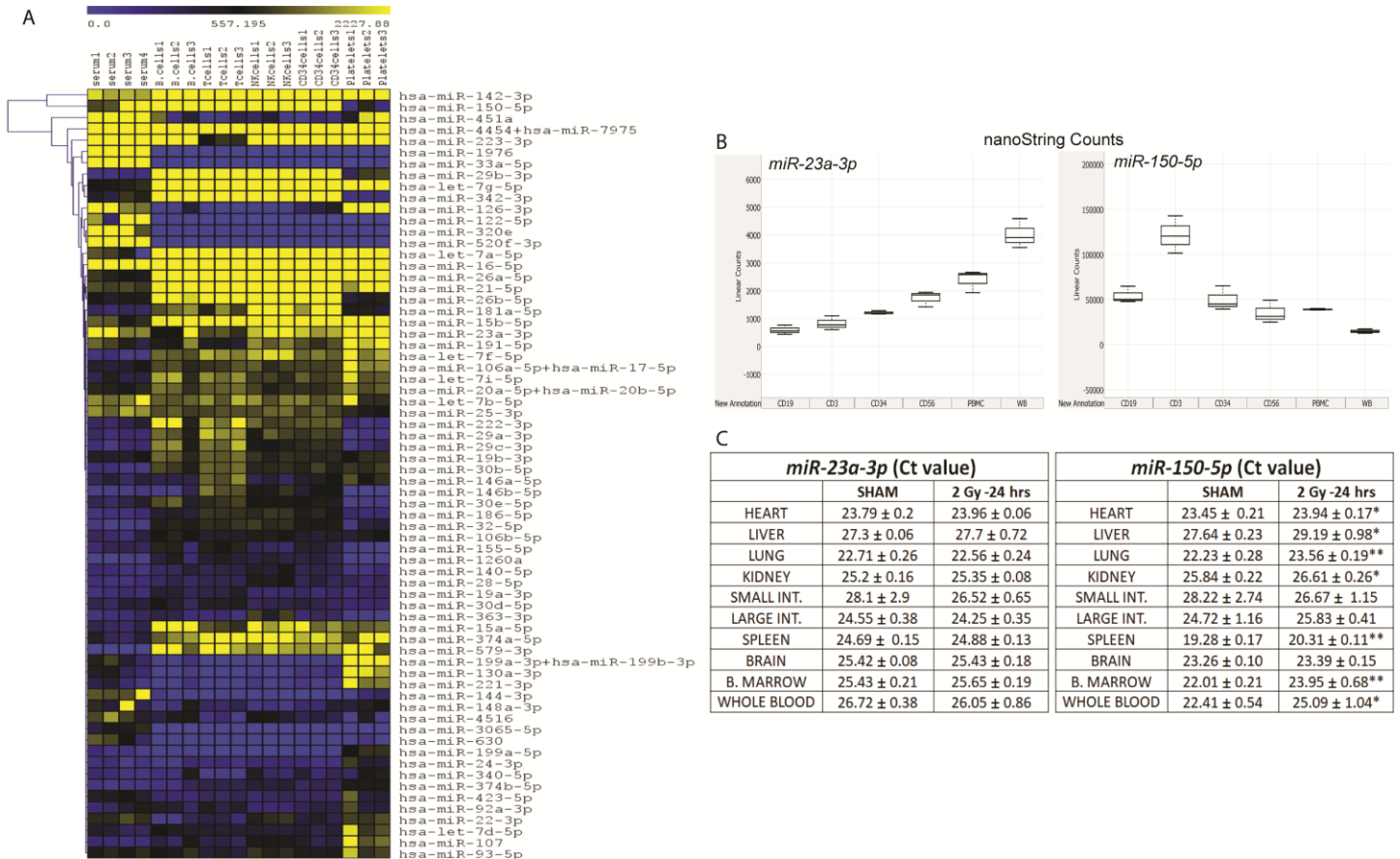


**Fig. S1. *miR-150-5p* and *miR-23a-3p* expression in human blood cell subsets, serum, and mouse tissues.** (A) Heat map summary and hierarchical clustering of top 65 miRNAs with counts  $\geq 400$  detected by nanoString nCounter technology based miRNA profiling of cell subsets from three different leukopaks and serum from healthy volunteers. Lower expression is represented in blue and higher expression in yellow. (B) Box plots show the comparison of the normalized nanoString counts of *miR-150-5p* and *miR-23a-3p* between each subset of peripheral blood mononuclear cells (PBMCs), and the whole blood (WB). (C) Ct value differences in *miR-150-5p* and *miR-23a-3p* (mean  $\pm$ SD of n=4 mice) in blood and various tissues collected from mice 24 hours after sham or 2 Gy TBI. Relatively high Ct denotes lower expression compared to low Ct values. Unpaired *t*-test \* $p < 0.05$ , \*\* $p < 0.01$ .

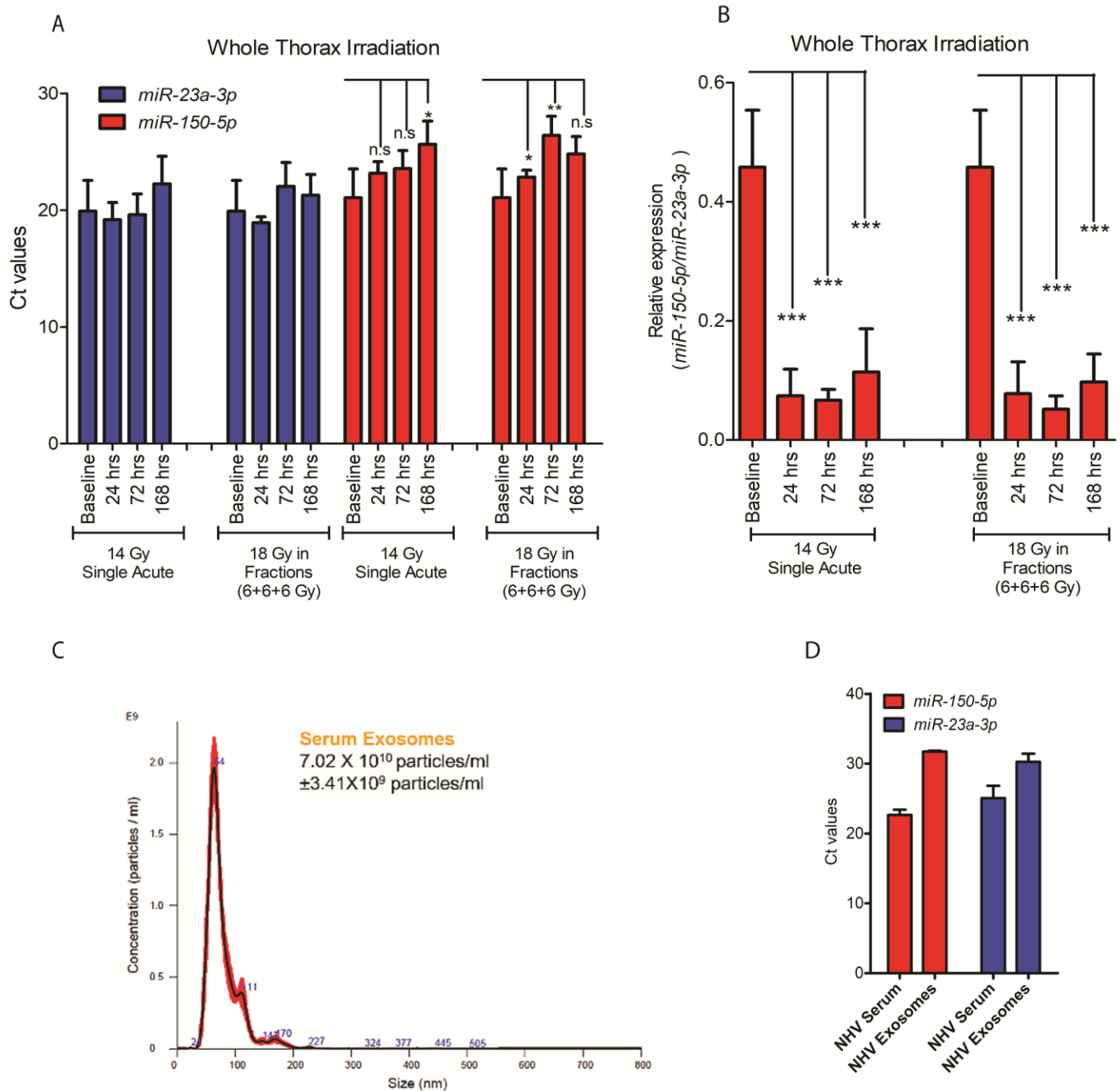


**Fig. S2. Normalizer *miR-23a-3p* is unaltered after exposure to high doses of whole thorax irradiation in mice and is secreted in nonexosomal fashion.** (A) Bar graph represents the Ct values of *miR-23a-3p* (blue) and *miR-150-5p* (red) from qRT-PCR using whole blood RNA purified from 18-24 month-old C57BL/6 mice at various time points after single dose (14 Gy) or fractionated (6+6+6 = 18 Gy) X-ray exposure targeted to the thorax. (B) Bar graph shows depletion of *miR-150-5p* (normalized with *miR-23a-3p*) until 72 hours and partial reconstitution by 168 hours. (C) NanoSight profile showing abundance of exosomes in healthy volunteers serum with peak at 64 nm (within the exosomes size range). (D) Bar graph represents the Ct value differences of *miR-150-5p* and *miR-23a-3p* between serum and exosomes purified from healthy volunteers serum. For data in (A) and (B), n=5/irradiation group, one-way ANOVA was applied, adjusted by Dunnett's method \* p<0.05, \*\*p<0.01, \*\*\*p<0.001.

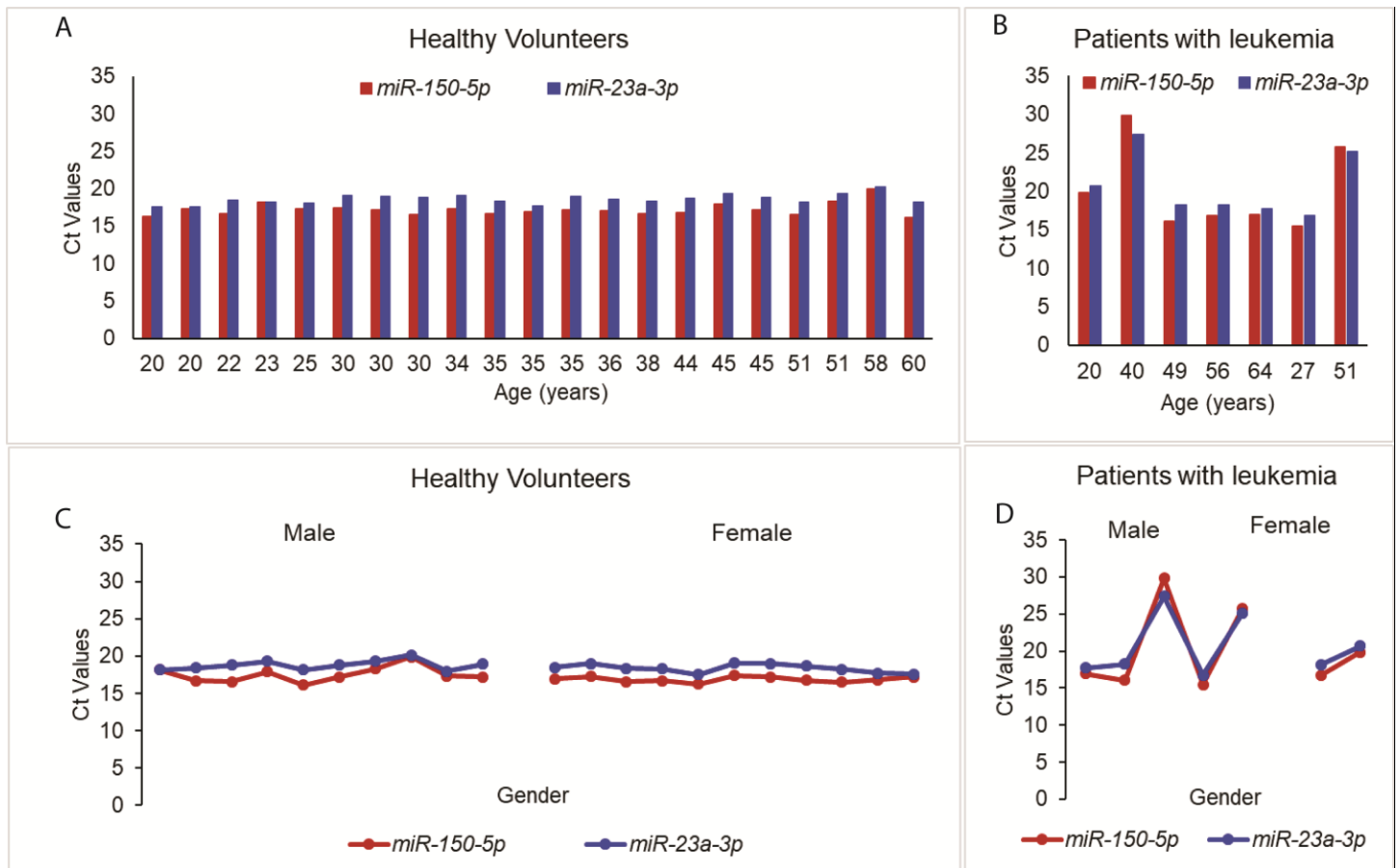


**Fig. S3. Finger-stick assay benchmarking according to gender and age at baseline in humans. (A)-(B),** Age- and (C)-(D), Sex- based comparison of *miR-150-5p* and *miR-23a-3p* in healthy volunteers and in patients with leukemia. For (A) and (C), healthy volunteers n=10 male and n=11 female; for (B) and (D), patients n=5 male and n=2 female.

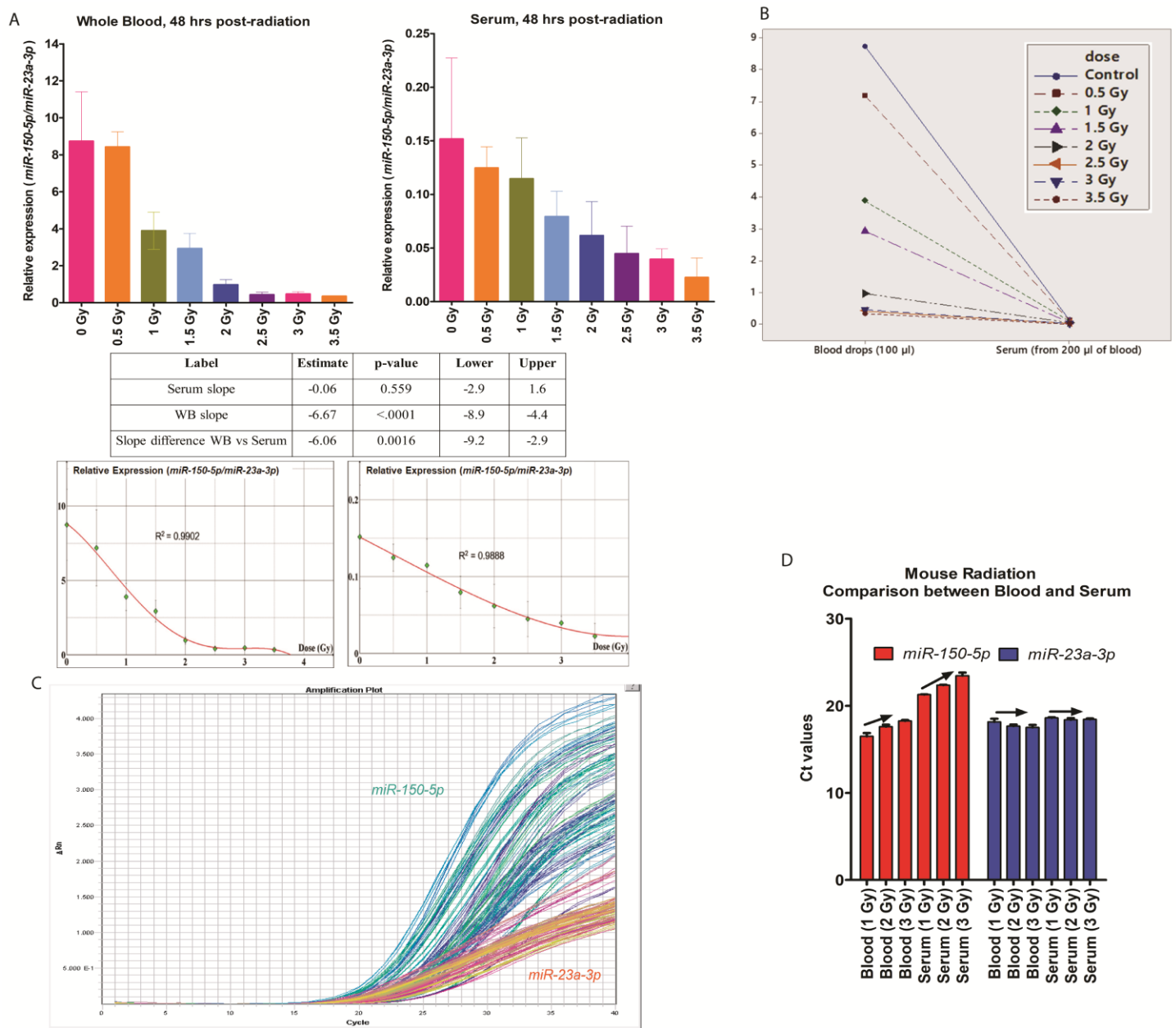


**Fig. S4. Comparison of dose response and sensitivity in mouse blood versus serum.** (A) Bar graph represents expression of *miR-150-5p* normalized to *miR-23a-3p*. Slopes of responses in whole blood and serum are  $-6.67/\text{Gy}$  and  $-0.06/\text{Gy}$ , respectively (difference= $-6.06/\text{Gy}$ , 95% confidence interval  $-2.9$ ;  $p$ -value $<0.0001$ , data were analyzed by ANOVA). (B) Dot-Line plot demonstrates better dose resolution and sensitivity measurable in blood, particularly at the lower dose range. Dot represents miR-RAD values of different gamma radiation doses, and lines represents the miR-RAD expression difference between blood drops and serum. (C) Snapshot of qPCR data plot of *miR-150-5p* (in blue and green hue) and *miR-23a-3p* (in red and yellow hue) showing similar range of expression at baseline in mouse blood. The *miR-150-5p* curves are more spread out than in the *miR-23a-3p* curves, indicating the dose-effect on *miR-150-5p*. The cycle number is represented on x-axis and  $\Delta R_n$  on y-axis. (D) Ct values of *miR-150-5p* and *miR-23a-3p* in blood and serum,  $n=5$  mice for each dose in blood and serum.

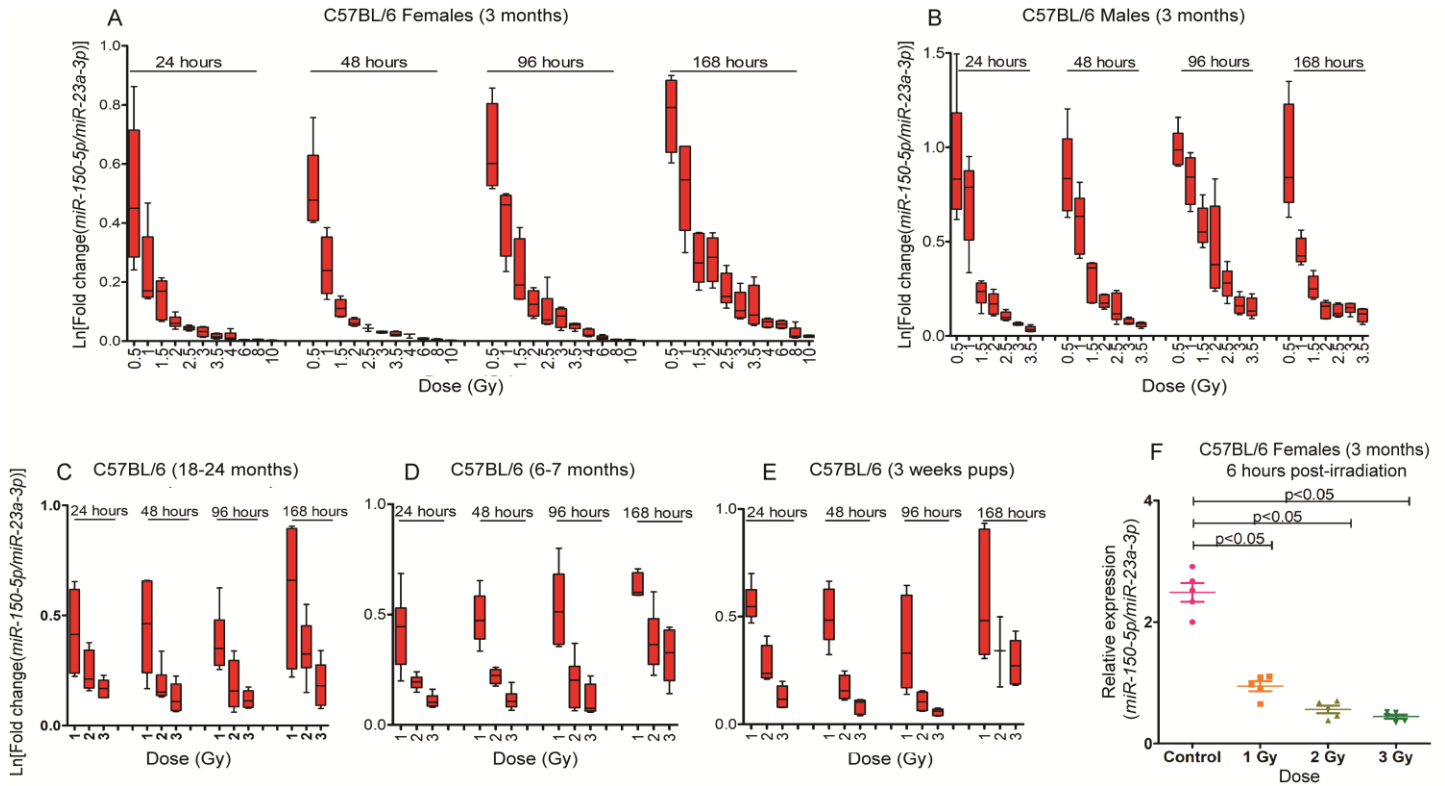


**Fig. S5. Longitudinal evaluation of dose response in pediatric, young-adult, middle-aged, and geriatric mice.** Box plots show the data obtained from longitudinal follow-up of *miR-150-5p* normalized to *miR-23a-3p* in mice exposed at various doses of TBI until 168 hours after irradiation. **(A)** 0.5-10 Gy in C57BL/6 females of 3-month old (young adult); **(B)** 0.5-3.5 Gy in C57BL/6 males of 3-month old (young adult); **(C)** 1-3 Gy in C57BL/6 male/females of 18-24 month old (geriatric); **(D)** 1-3 Gy in C57BL/6 male/females of 6-7 month old (middle-aged); **(E)** 1-3 Gy in C57BL/6 male/females of 3-week old (pediatric) collected at 24, 48, 96, and 168 hours after irradiation. **(F)** Dot plot showing response at 6 hours post-irradiation in 3-month-old C57BL/6 female mice (n=5). For **(F)** one-way ANOVA was applied, adjusted by Dunnett's method p<0.05 is significant.



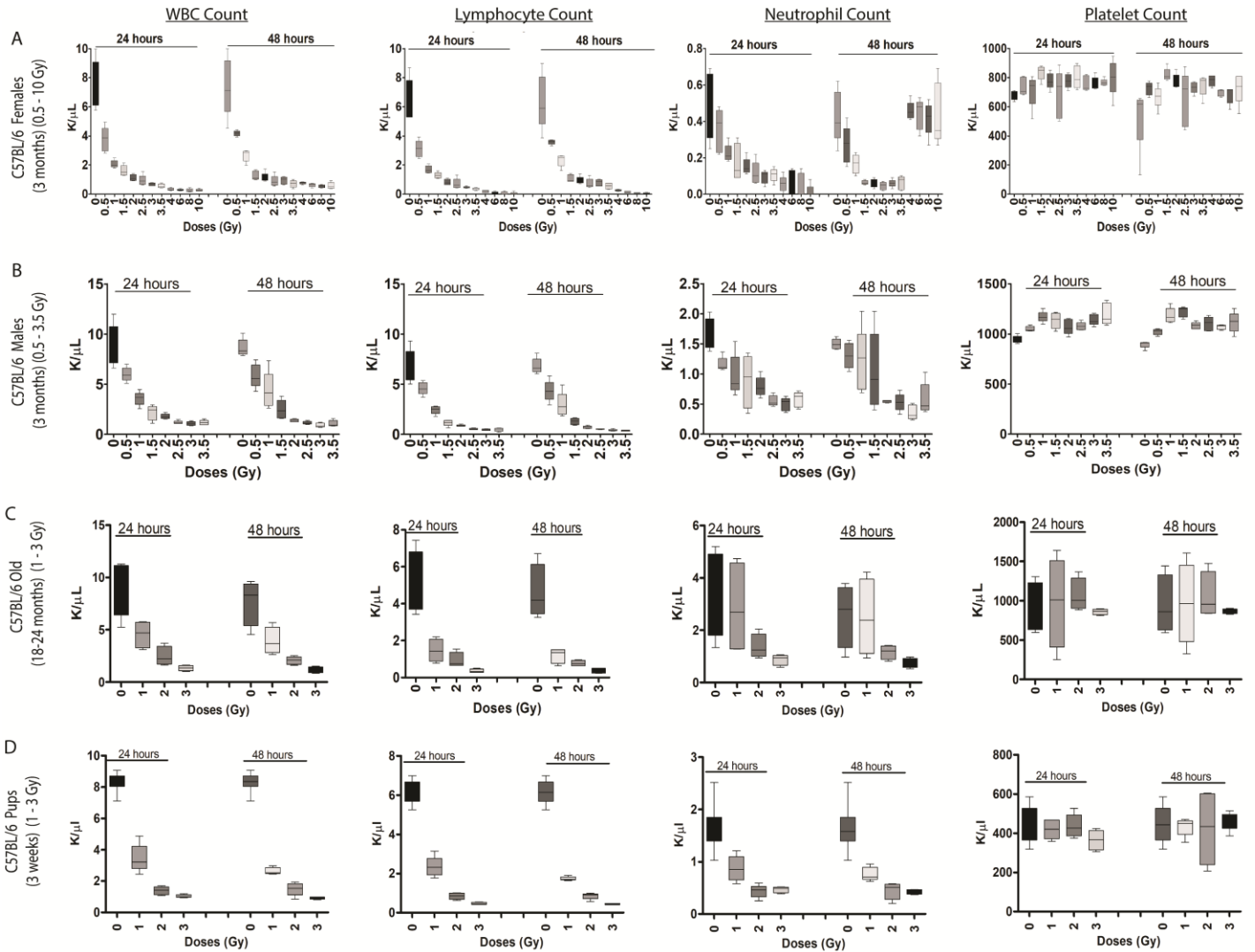


**Fig. S6. CBC in mice of different ages after exposure to a broader dose range.** Box plots showing changes in whole white blood cells, lymphocyte, neutrophil, and platelet count after exposure to varying doses of TBI. (A) 0.5-10 Gy in C57BL/6 females of 3-month old (young adult); (B) 0.5-3.5 Gy in C57BL/6 males of 3-month old (young adult); (C) 1-3 Gy in C57BL/6 male/females of 18-24 month old (geriatric); (D) 1-3 Gy in C57BL/6 male/females of 3-week old (pediatric) collected at 24 and 48 hours post-irradiation.

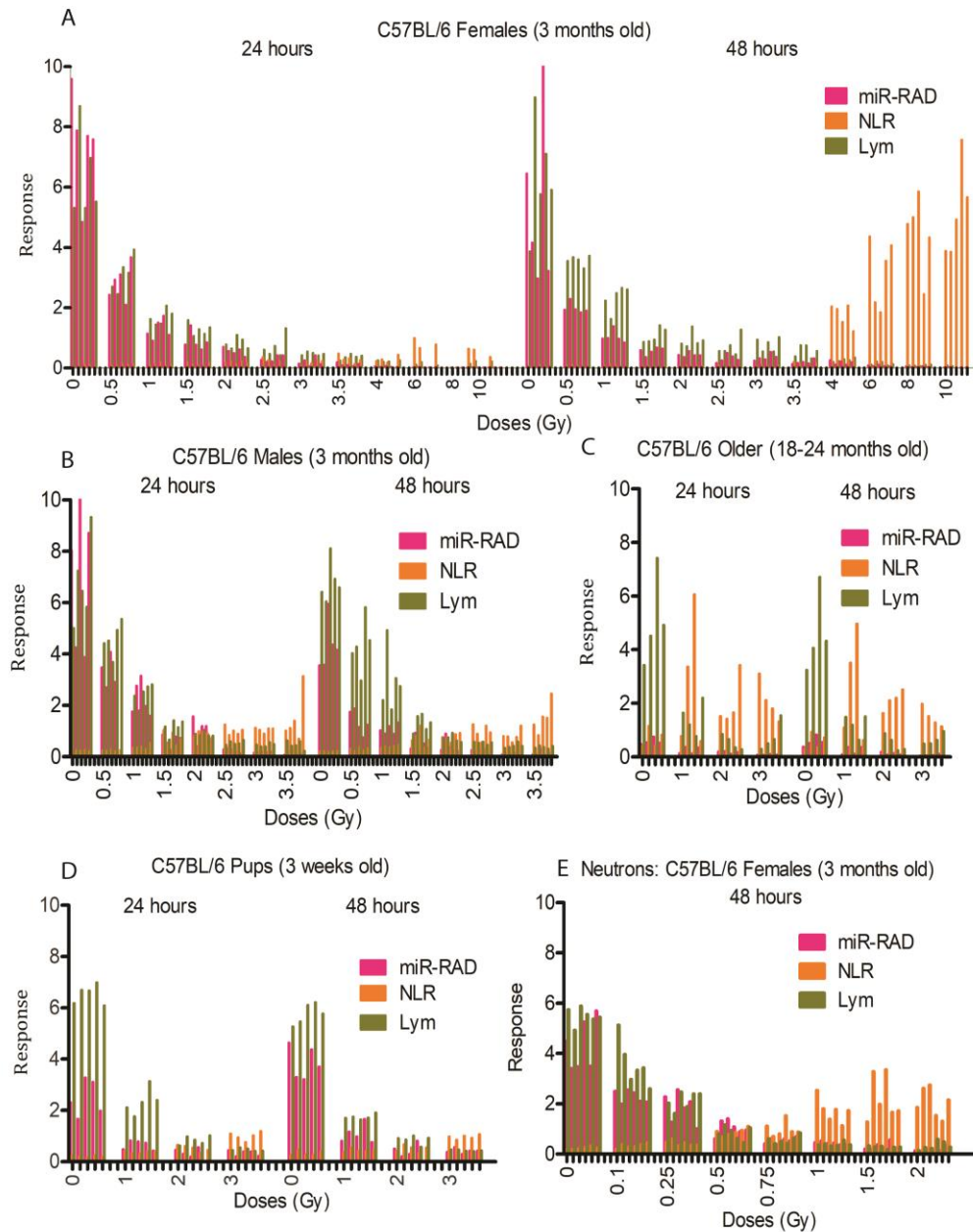


**Fig. S7. Comparison of miR-RAD with lymphocyte depletion and NLR.** Histograms shows sensitivity of miR-RAD in comparison to depletion of lymphocytes ( $K/\mu l$ ) (Lym), and neutrophil to lymphocyte ratio (NLR) at 24 and 48 hours after total body gamma (A-D) or neutron (E) irradiation. (A) 0.5-10 Gy gamma rays in C57BL/6 females of 3-month old ( $n=5$ ); (B) 0.5-3.5 Gy gamma rays in C57BL/6 males of 3-month old ( $n=5$ ); (C) 1-3 Gy gamma rays in C57BL/6 male/females of 18-24 month old ( $n=4$ ); (D) 1-3 Gy gamma rays in C57BL/6 males/females of 3-week old ( $n=5$ ), (E) 0.1-2 Gy neutrons in C57BL/6 females of 3-month old ( $n=6$ ).

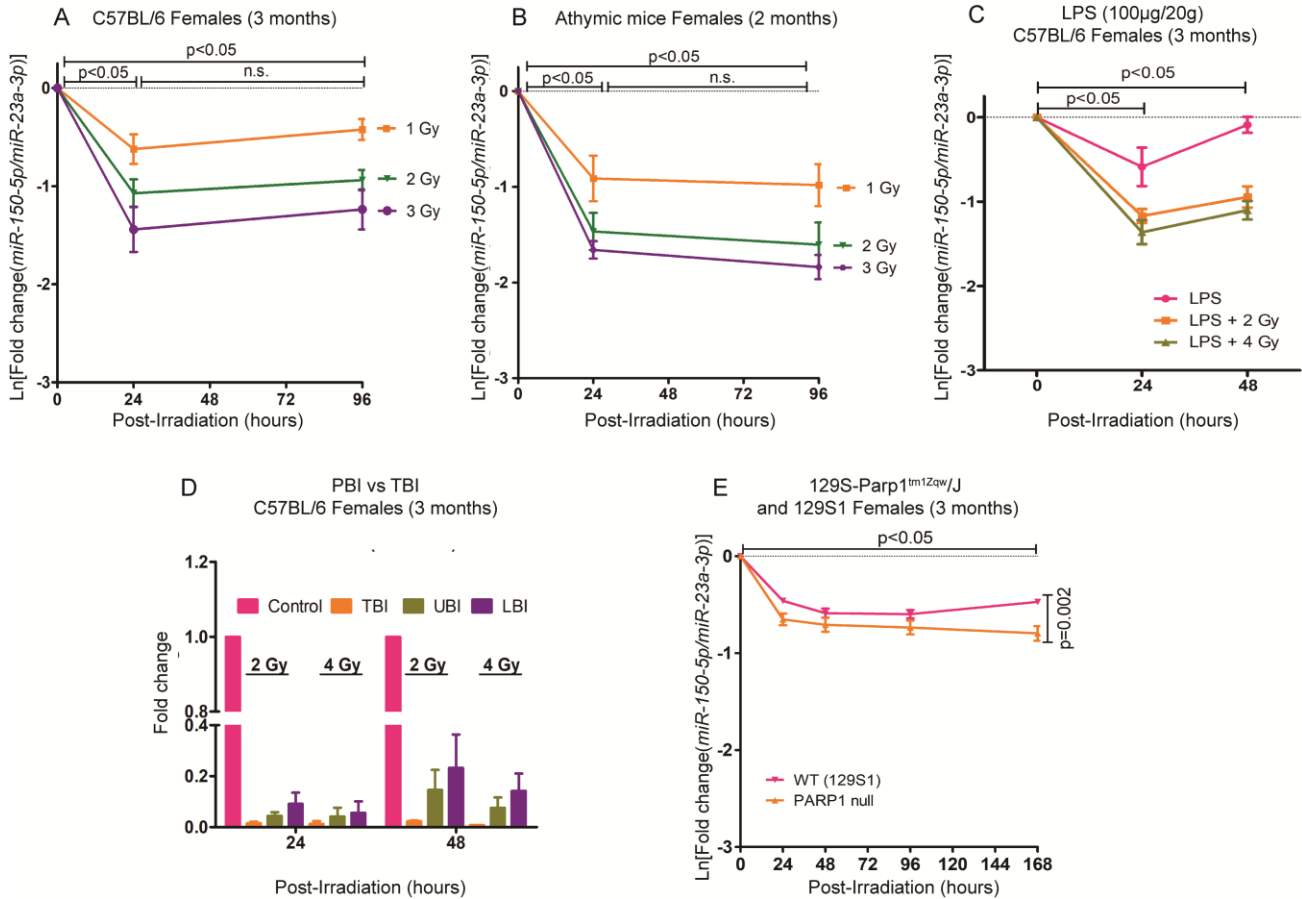


**Fig. S8. Dose response in immunocompetent, immunocompromised, immune-challenged, partial body exposure, and DNA repair-deficient mice.** (A)-(B) Dose-time response in three-month-old C57BL/6 (immune-competent) and athymic (NCr-nu/nu) immuno-deficient mice exposed to 1, 2, and 3 Gy TBI, evaluated at 24 and 96 hours (n=5 for each dose). (C) The dose-time response in 3-month-old C57BL/6 female mice exposed to a high dose of bacterial endotoxin lipopolysaccharide (5mg/kg, *i.p.*) and TBI (2 and 4 Gy). (D) Fold change of *miR-150-5p* normalized to *miR-23a-3p* after total body irradiation (TBI, 100% marrow exposure), upper body irradiation (UBI, about 60% marrow exposure), and lower body irradiation (LBI, about 40% marrow exposure) (n=5). (E) Dose-time response in PARP1 null (129S-Parp1<sup>tm1Zqw/J</sup>) or WT in 129S1 background 3-month-old female mice (n=5) after total body exposure to 2 Gy. For (A-C) and (E) one-way ANOVA was applied, adjusted by Dunnett's method. p<0.05 is significant and n.s. is not significant.

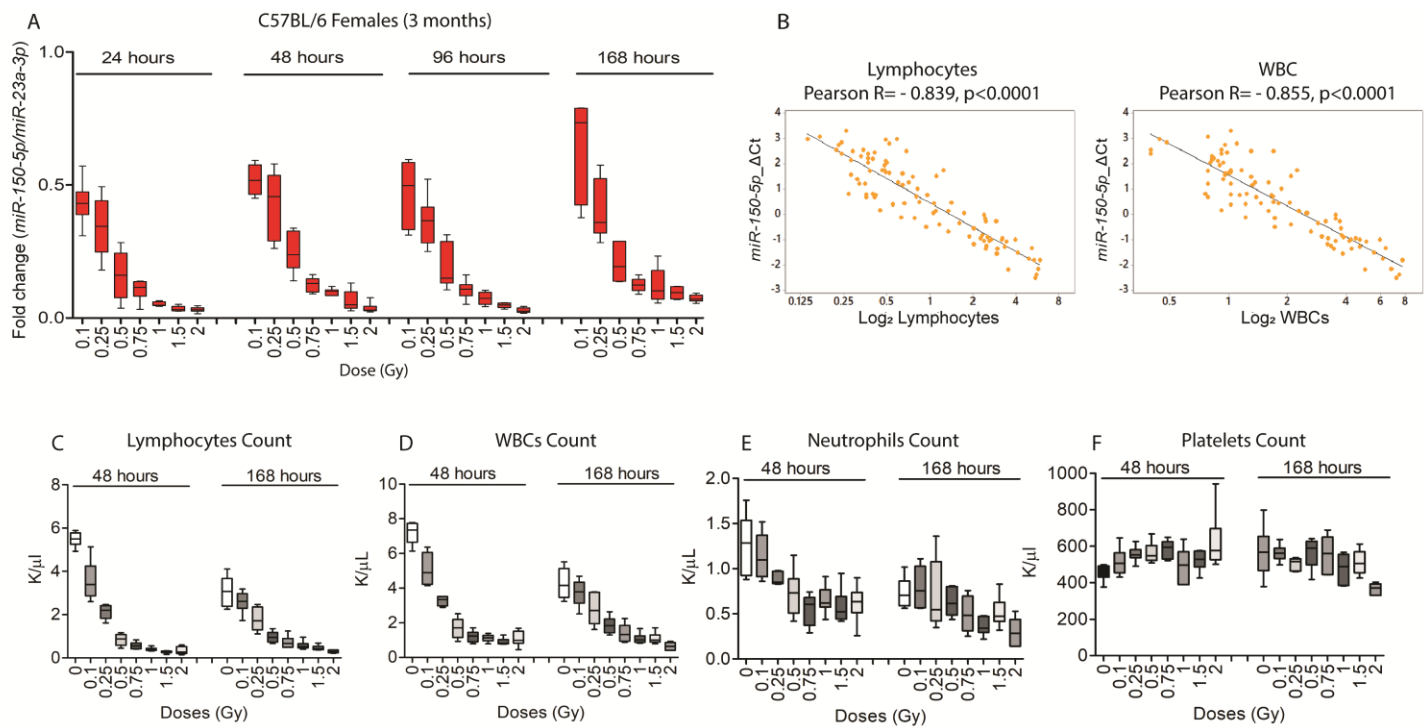


**Fig. S9. miR-RAD with CBC analysis after neutron irradiation in mice.** (A) Box plots represent the data obtained after longitudinal follow-up of miR-RAD post 0.1-2 Gy neutrons in C57BL/6 females of 3-month old mice. (B) Scatter plots demonstrate Pearson correlation between *miR-150-5p* and lymphocytes or white blood cells (WBCs); y-axis shows  $\Delta$ Ct values obtained from *miR-150-5p* normalized to *miR-23a-3p* while in x-axis  $\log_2$ (lymphocytes count) or  $\log_2$ (WBC count) is shown. Box plots representing lymphocytes (C), white blood cells (D), neutrophil (E), and platelet (F) counts. n=6 animals/dose normalized with unirradiated sham controls at respective time points.

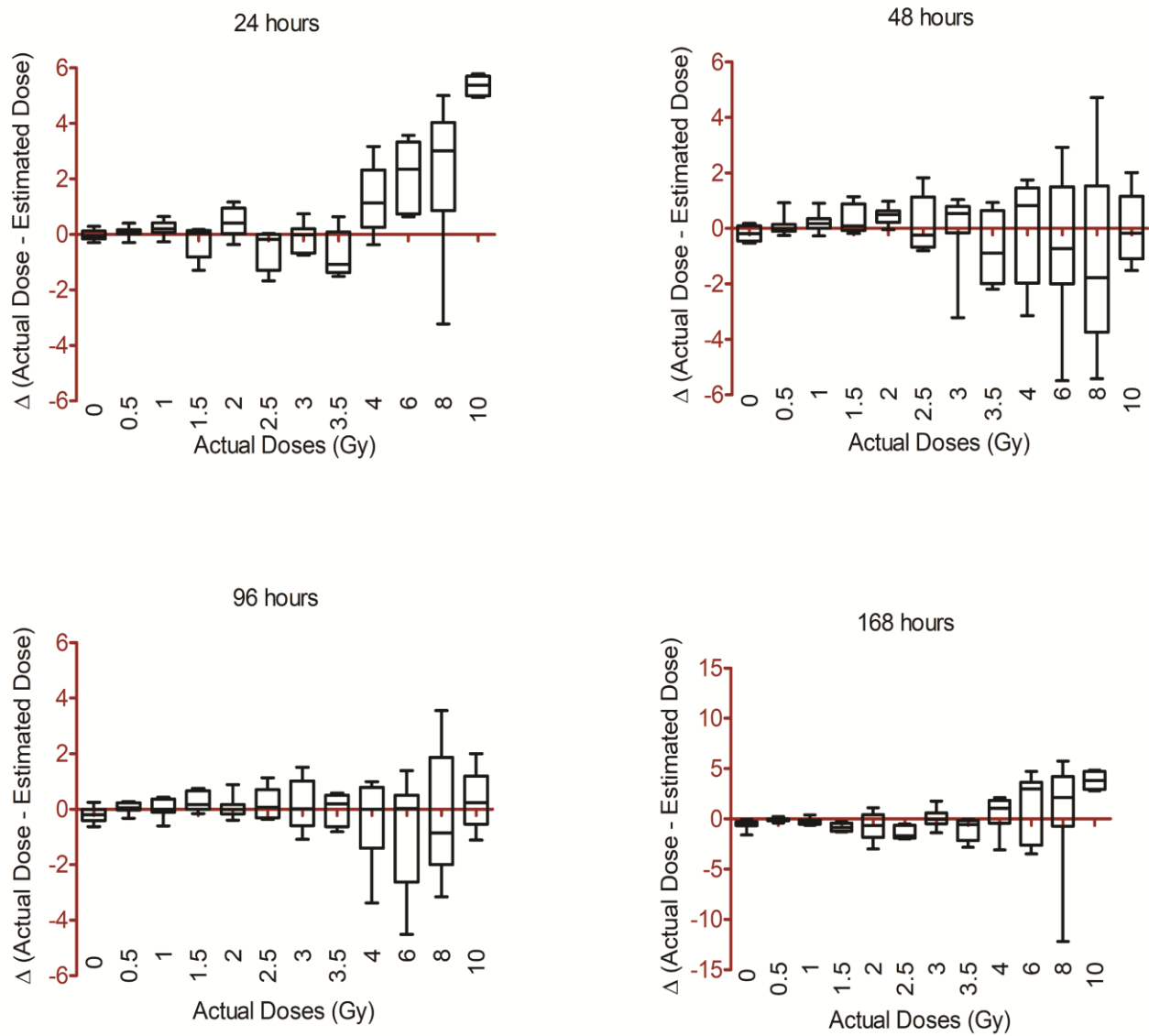


**Fig. S10. An overview of the accuracy of miR-RAD in a broad dose range.** Box plots shows the range of estimated doses based on prediction algorithms at various time points. Deviation is calculated by subtracting estimated dose from the actual dose represented as mean  $\pm$ SD.

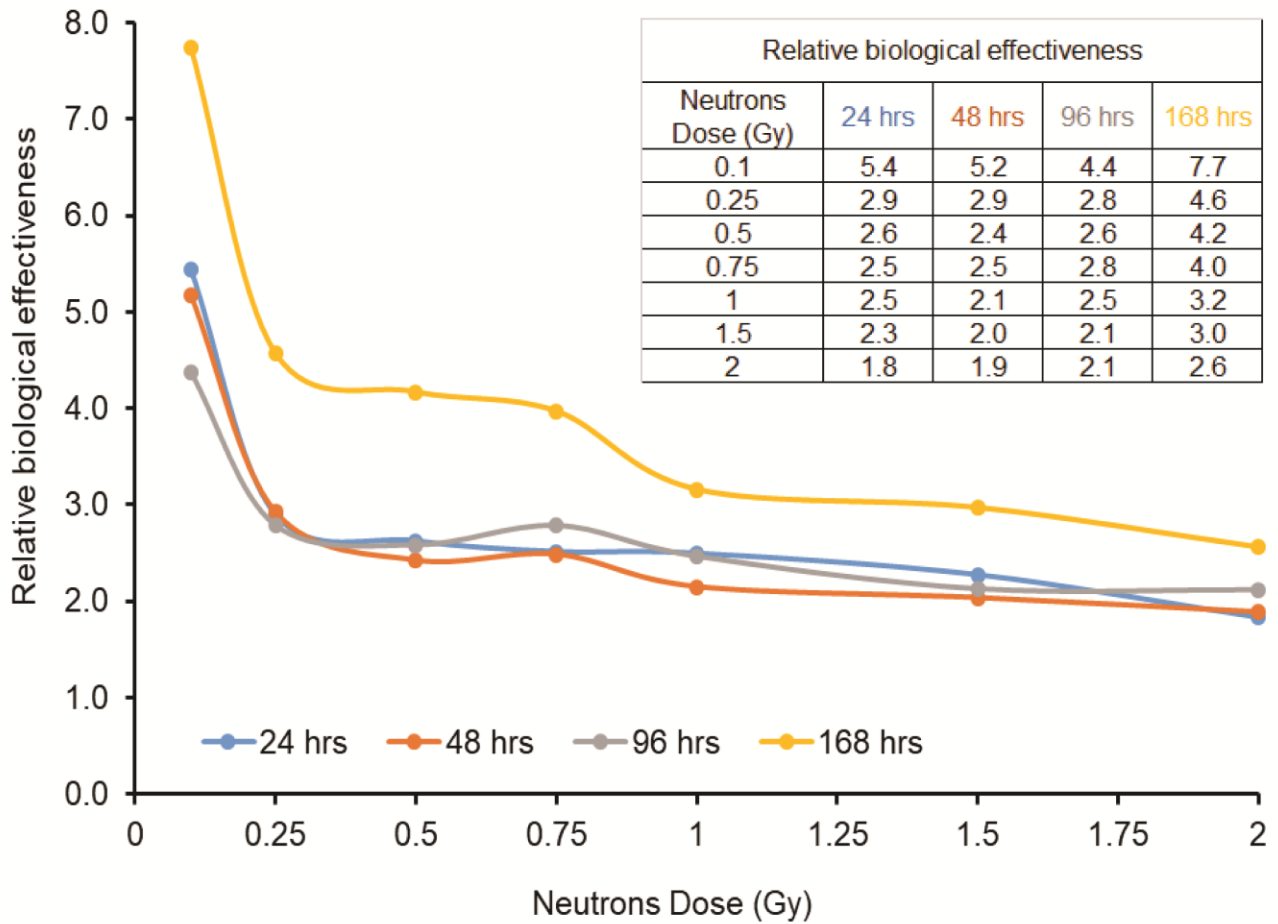


**Fig. S11. Relative biological effectiveness of neutron with miR-RAD endpoint.** Relative biological effectiveness values were calculated at various time points using prediction algorithms generated from mice exposed to <sup>137</sup>Cs gamma rays.

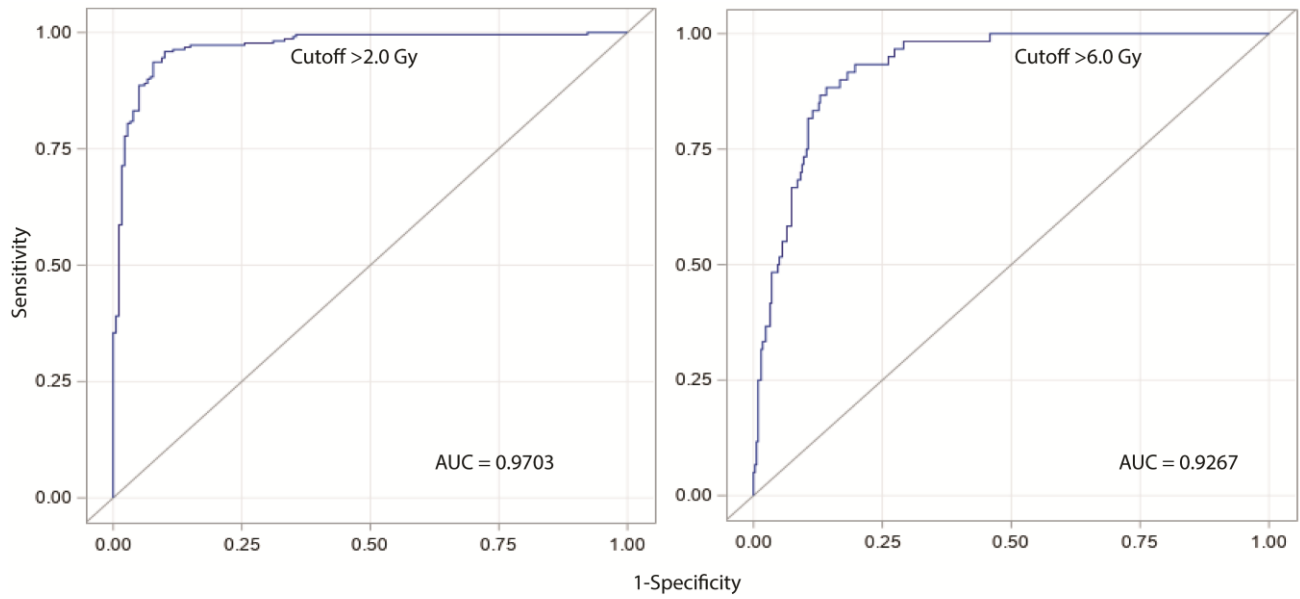


**Fig. S12. ROC curves for absorbed dose >2 or >6 Gy using miR-RAD.** ROC curves demonstrate AUC values of 0.97 and 0.93 for actual absorbed dose >2.0 Gy or >6.0 Gy respectively using combined 3-month-old male and female mice data from 24, 48, 96, and 168 hours with 400 data points.

**Table S1. Baseline  $C_t$  values of *miR-150-5p* and *miR-23a-3p* in finger-stick blood from healthy volunteers and venous blood from patients with leukemia.  $C_t$  values of *miR-150-5p* and *miR-23a-3p* obtained by an advanced high sensitive qRT-PCR assay and  $\Delta\Delta C_t$  derived from healthy volunteers (NHVs, n=21) and patients with leukemia (n=7).**

Sample ID (Healthy Volunteers)	Gender	Age	Ethnicity	Under Chronic Medication	Ct value		$\Delta\Delta C_t$
					<i>miR-150-5p</i> -FAM	<i>miR-23a-3p</i> -FAM	
NHV01	F	36	South Asian	No	16.97	18.51	2.90
NHV02	M	23	East Asian	No	18.18	18.15	0.97
NHV03	F	34	Caucasian	No	17.25	19.02	3.40
NHV04	F	38	Caucasian	Anti-Hypertensive	16.59	18.33	3.35
NHV05	F	35	Caucasian	No	16.70	18.27	2.98
NHV06	F	20	South Asian	No	16.23	17.52	2.45
NHV07	M	22	East Asian	No	16.67	18.42	3.35
NHV08	M	30	South Asian	No	16.55	18.81	4.79
NHV09	M	45	African	No	17.89	19.32	2.71
NHV10	F	30	Hispanic	No	17.37	19.05	3.20
NHV11	M	60	South Asian	Anti-Diabetic	16.12	18.18	4.17
NHV12	M	45	Caucasian	Anti-Hypertensive	17.17	18.82	3.14
NHV13	F	30	South Asian	No	17.18	18.97	3.45
NHV14	M	51	South Asian	Statins	18.31	19.29	1.96
NHV15	F	44	South Asian	Anti-Thyroid	16.77	18.70	3.80
NHV16	M	58	East Asian	Anti-Hypertensive	19.89	20.16	1.21
NHV17	F	51	South Asian	Antibiotic	16.48	18.21	3.33
NHV18	F	35	South Asian	Anti-Diabetic	16.83	17.69	1.82
NHV19	M	25	Caucasian	No	17.33	17.99	1.58
NHV20	M	35	Caucasian	No	17.19	18.93	3.34
NHV21	F	20	South Asian	No	17.22	17.58	1.28

Sample ID	Gender	Age	Disease	Ct value		$\Delta\Delta C_t$
				<i>miR-150-5p</i> -FAM	<i>miR-23a-3p</i> -FAM	
Patient 1	M	64	MDS	16.96	17.72	1.69
Patient 2	M	49	ALL	16.05	18.21	4.48
Patient 3	F	56	ALL	16.78	18.20	2.67
Patient 4	F	20	ALL	19.84	20.66	1.77
Patient 5	M	40	ALL	29.83	27.39	0.18
Patient 6	M	27	AML	15.47	16.79	2.49
Patient 7	M	51	CML/ALL	25.78	25.10	0.63



**Table S2. Overview of mouse samples including number of animals and sampling time points.** The table provide an overview of experimental studies, number of animals, and collection time points.

Experiment Study	Number of animals/dose	Animals/Longitudinal Follow-Up	Samples Processed	Radiation Type
C57BL/6 Females 3 mo. old (Young-adult)	5/(0-10 Gy)   0-4 Gy $\pm$ 0.5 Gy   6-10 Gy $\pm$ 2 Gy	60x 24, 48, 96, and 168 hrs	240	Gamma
C57BL/6 Males 3 mo. old (Young-adult)	5(0-3.5 Gy)   0-3.5 Gy $\pm$ 0.5 Gy	40x 24, 48, 96, and 168 hrs	160	Gamma
C57BL/6 6-7 mo. old (Middle-aged)	6(0-3 Gy)   0, 1, 2, 3 Gy	24x 24, 48, 96, and 168 hrs	96	Gamma
C57BL/6 18-26 mo. old (Geriatric)	4/(0-3 Gy)   0, 1, 2, 3 Gy	16x 24, 48, 96, and 168 hrs	64	Gamma
C57BL/6 pups 3 wk. old (Pediatric)	5/(0-3 Gy) + 5(0-3 Gy)   0, 1, 2 and 3 Gy	40x 24, 48, 96, and 168 hrs	160	Gamma
Athymic mice (NCR-nu/nu)	5/(0-3 Gy)   0, 1, 2, 3 Gy	20x 24 and 96 hrs	40	Gamma
Partial Body Irradiation (UBI, LBI, TBI), C57BL/6 Females 3 mo. old	5/(2 and 4 Gy)/group	35x 24 and 48 hrs	70	X-ray
LPS and Irradiation, C57BL/6 Females 3 mo. old	5/(2 and 4 Gy)/group	20x 24 and 48 hrs	40	Gamma
Identification of miR-23a source- C57BL/6 Females 3 mo. old	4/(0 and 2 Gy)	8 (different organs)	78	Gamma
Distinguishing unexposed vs 2 Gy C57BL/6	5/each age group	25x 24 hrs	25	Gamma
Whole Thorax IR, C57BL/6 Male and Females 18-24 mo. old	5/(Sham, Acute IR and fractionated IR)	15x 24, 72, and 168 hrs	45	X-ray
C57BL/6 Females 10 wk. old	5/(0 and 2 Gy)	5x 24, 48, 96, and 168 hrs	20	Gamma
129S1 Females 10 wk. old	5/(0 and 2 Gy)	5x 24, 48, 96, and 168 hrs	20	Gamma
129S-Parp1tm1Zqw/J Females 10 wk. old	5/(0 and 2 Gy)	5x 24, 48, 96, and 168 hrs	20	Gamma
Early response, C57BL/6 3 mo. old	5/(1-3 Gy)   0, 1, 2 and 3 Gy	20x 6 hrs	20	Gamma
Prediction algorithms, C57BL/6 Females 3 mo. old	2*5/(0-10 Gy)   0-4 Gy $\pm$ 1Gy   6-10 Gy $\pm$ 2 Gy	77x 24, 80x 48, 80x 96, and 79x168 hrs	316	Gamma
Dose Reconstruction Blinded, C57BL/6 Male and Females 3 mo. old	2*5/(0.5-10 Gy)   0-4 Gy $\pm$ 0.5 Gy   6-10 Gy $\pm$ 2 Gy	60x 24, 48, 96, and 168 hrs	240	Gamma
Dose Reconstruction-Repeat and RBE Ref-Gamma, C57BL/6 Females 3 mo. old	5/(0, 0.5, 1, 2, 3, 4, 6, and 8 Gy)	40x 24, 48, 96, and 168 hrs	160	Gamma
C57BL/6 Females (RBE Neutron) 3 mo. old	6/(0, 0.1, 0.25, 0.5, 0.75, 1, 1.5 and 2 Gy)	48x 24, 48, 96, and 168 hrs	192	Neutron
Bridging study- Fractionated TBI, C57BL/6 Females 3 mo. old	8/(Sham, 1 and 2 Gy BID)	24x 24 hrs; 16x 48, 96 and 120 hrs; 14x 168 hrs; 6-10x week 2-4 without/with transplant (2 Gy BID); 8x week 2-4 (1 Gy BID)	166	Gamma
<b>Total</b>	<b>535</b>		<b>2172</b>	

**Table S3. Overview of human samples used for dose-response evaluation and controls.** The table shows the number of volunteers and patients under various protocols with sampling time points.

<b>Clinical Study</b>	<b># of patients and time-points</b>	<b># of samples processed</b>
NCT02122081 (OSU-13219) – patient whole blood and serum comparison – Fig. 2D-E	4x (baseline, D-5, D-4, D-2, D-1) + 4x (D+30)	24 whole blood and 24 serum
NCT02122081 (OSU-13219) – patient serum- Fig. 2A	6x (baseline, D-4, D-1) + 4x (D+30)	22 serum
NCT02122081 (OSU-13219) – patient serum – Fig. 2B	7x (baseline, D-5, D-4, D-2, D-1, D+30)	42 serum
NCT01521039 (OSU-11002)- patient serum- Validation – Fig. 2C	7x (baseline, D-1, D+30)	21 serum
NCT02122081 (OSU-13219)- patients whole blood long term follow-up – Fig. 2F	6x (D+365) + 3x (D+180) + 4x (D+30) + 4x (baseline)	9 whole blood (A total of 30 early time points of these pts are included above)
NCT02122081 (OSU-13219)- patients whole blood – Fig. 6A, B, and D	3x (baseline, D-5, D-4, D-2, D-1, D+30)	18 whole blood (24 whole blood samples from above were also included for a total of 7 pts samples)
Healthy Volunteers (NHVs) (OSU2016C0032)	27 (male and female with varying age/ethnicity including individuals with underlying chronic conditions)	21 Finger-stick + 6 venous blood collection
<b>Total</b>		<b>187</b>

**Table S4. Comparison of uncertainty error with  $\Delta\Delta C_t$  versus normalized  $\Delta\Delta C_t$  in mice.**

C57BL/6 Females - 3 months old								Relative fold error reduction		
Time-point	Dose (Gy)	$\Delta\Delta C_t =$ miR-150 - miR-23a	$\sigma$	$\sigma/\text{Avg}(\%)$	$\Delta\Delta C_t$ normalized = [(miR-150 - miR-23a)/ miR- 23a]	$\sigma$	$\sigma / \text{Avg} (\%)$	Ratio of [ $\sigma/\text{Avg}(\%)$ ]/[ $\sigma/\text{Avg}$ (%)]	Mean	S.D.
24 hours	0	9.313	0.949	10.192	1.105	0.007	0.606	16.81	17.44	2.295851
	1	2.890	0.597	20.649	1.042	0.011	1.036	19.94		
	2	0.704	0.090	12.777	0.980	0.006	0.590	21.67		
	3	0.261	0.040	15.484	0.930	0.010	1.106	14.01		
	4	0.109	0.023	20.751	0.891	0.011	1.279	16.22		
	6	0.045	0.010	21.807	0.851	0.012	1.412	15.45		
	8	0.029	0.008	25.627	0.835	0.012	1.476	17.36		
	10	0.027	0.006	24.288	0.826	0.011	1.342	18.10		
48 hours	0	5.429	0.755	13.914	1.087	0.008	0.764	18.22	17.77	4.738128
	1	1.237	0.115	9.318	1.009	0.005	0.452	20.62		
	2	0.526	0.116	22.044	0.960	0.007	0.767	28.76		
	3	0.318	0.043	13.561	0.937	0.008	0.835	16.25		
	4	0.162	0.023	14.424	0.902	0.008	0.850	16.98		
	6	0.064	0.008	12.131	0.861	0.008	0.879	13.80		
	8	0.039	0.006	14.962	0.835	0.009	1.088	13.76		
	10	0.021	0.003	15.068	0.805	0.009	1.092	13.80		
96 hours	0	3.475	0.770	22.160	1.053	0.012	1.149	19.29	16.11	3.789478
	1	0.913	0.178	19.544	0.988	0.008	0.857	22.81		
	2	0.487	0.081	16.685	0.956	0.009	0.971	17.18		
	3	0.269	0.058	21.510	0.919	0.012	1.323	16.26		
	4	0.105	0.026	24.676	0.865	0.014	1.658	14.89		
	6	0.051	0.011	21.443	0.832	0.013	1.585	13.53		
	8	0.036	0.007	19.585	0.812	0.018	2.175	9.01		
	10	0.025	0.006	24.605	0.807	0.012	1.543	15.94		
168 hours	0	5.838	1.310	22.446	1.081	0.008	0.753	29.81	21.12	3.759337
	1	1.836	0.622	33.864	1.012	0.015	1.497	22.63		
	2	0.909	0.191	21.000	0.984	0.011	1.151	18.24		
	3	0.483	0.084	17.422	0.960	0.008	0.830	20.98		
	4	0.283	0.035	12.446	0.938	0.006	0.692	17.97		
	6	0.238	0.044	18.425	0.925	0.008	0.880	20.94		
	8	0.126	0.017	13.564	0.898	0.007	0.797	17.01		
	10	0.108	0.028	26.362	0.887	0.011	1.233	21.38		

**Table S5. Tabulation of actual dose versus estimated dose in mice.**

<b>Actual Dose (Gy)</b>	<b><math>\Delta</math> (Actual-Estimated dose)</b>	<b>Stdv</b>
0	-0.242	0.350
0.5	0.021	0.175
1	0.015	0.339
1.5	-0.152	0.622
2	-0.013	0.864
2.5	-0.541	0.824
3	0.083	1.027
3.5	-0.546	1.038
4	0.182	1.596
6	0.593	2.616
8	1.246	3.409
10	2.140	2.271

**Table S6. Tabulation of assay sensitivity and specificity at 0.5, 2, and 6 Gy cutoff.** The cutoffs for miR-RAD sensitivity and specificity determined from data points generated from dose calculation.

	<b>Actual Dose 0-0.5 Gy</b>	<b>Actual Dose</b>	<b>SUM</b>
		<b>0.5-10.0 Gy</b>	
miR-RAD 0-0.5 Gy	53	2	55
miR-RAD >0.5 Gy	27	318	345
<b>SUM</b>	<b>80</b>	<b>320</b>	<b>400</b>

Sensitivity:  $318/320=99.38\%$ ; Specificity:  $53/80=66.25\%$

	<b>Actual Dose 0-2.0 Gy</b>	<b>Actual Dose</b>	<b>SUM</b>
		<b>2.0-10.0 Gy</b>	
miR-RNA 0-2.0 Gy	160	9	169
miR-RNA >2.0 Gy	20	211	231
<b>SUM</b>	<b>180</b>	<b>220</b>	<b>400</b>

Sensitivity:  $211/220=95.91\%$ ; Specificity:  $160/180=88.9\%$

	<b>Actual Dose 0-6.0 Gy</b>	<b>Actual Dose</b>	<b>SUM</b>
		<b>6.0-10.0 Gy</b>	
miR-RNA 0-6.0 Gy	321	27	348
miR-RNA >6.0 Gy	19	33	52
<b>SUM</b>	<b>340</b>	<b>60</b>	<b>400</b>

Sensitivity:  $33/60=55\%$ ; Specificity:  $321/340=94.4\%$